Sensors and Materials, Vol. 36, No. 1 (2024) 127–133
MYU Tokyo

S & M 3502

Effects of Printing Angle on Mechanical Characteristics of Resin Castable Wax V1

Pham Thi Hong Nga,* Tran Minh Truong, Tran Khanh Tuyen, Pham Thanh Tam, Do Thi Le Mai, Nguyen Thanh Tan, Hoang Van Huong, Nguyen Van Thuc, Nguyen Khac Nhan, Ho Sy Hung, and Tran The San

Faculty of Mechanical Engineering, Ho Chi Minh City University of Technology and Education, No. 1 Vo Van Ngan Street, Linh Chieu Ward, Thu Duc City, Ho Chi Minh City 71307, Vietnam

(Received May 31, 2023; accepted January 5, 2024)

Keywords: additive manufacturing, SLA, printing angle, tensile strength, compressive strength

Material additive or 3D printing technology has been recognized as a future manufacturing technique. The mechanical properties of products manufactured using 3D printing technology depend on many factors, especially the printing angle. Resin Castable Wax can be used as a matrix or scaffold for sensor devices in 3D printing. In this study, we explore the effects of printing angle on the mechanical properties of Resin Castable Wax V1 using the 3D stereolithography printing method. The samples are printed at three different printing angles of 0, 45, and 90°. Increasing the printing angle from 0 to 90° improves the tensile and compressive strengths. The sample printed at the angle of 90° shows the highest ultimate tensile and compressive strengths of 23.13 and 124.97 MPa, respectively, and vice versa for the sample printed at 0º. Because of the gradual inclination of the material toward the direction of load force and the larger printing boundary at a higher printing angle, the mechanical properties are improved when the printing angle is increased. These findings can be used to choose an appropriate printing angle for Resin Castable Wax V1.

1. Introduction

Recently, the increasing demand for highly accurate and complex printed products has made 3D printing technology increasingly popular. The reason is its flexibility and ability to manufacture complex parts compared with traditional manufacturing processes.(1) 3D printing technology began with the development of standard tessellation language (STL), which is constructed using computer-aided design (CAD) software to create 2D slice building data. This 2D data is sent to the 3D printer. To create a 3D printing component, various techniques such as digital light processing (DLP), continuous liquid interface production (CLIP), selective laser sintering (SLS), fused filament fabrication (FDM), and stereolithography (SLA) have been developed. Each of these techniques has its own set of drawbacks, benefits, and applications.(2)

*Corresponding author: e-mail: hongnga@hcmute.edu.vn
https://doi.org/10.18494/SAM4536

ISSN 0914-4935

Among the above-mentioned techniques, the SLA technique invented in 1980 by Kodama is widely used.[3] This method uses a special photopolymer resin. When the SLA resin is subjected to a specific wavelength of light, short chains of molecules bond with each other, polymerizing monomers and oligomers into hard or resinous objects.[4,5] The SLA technique can be used for different applications such as medical modeling, presurgical planning, designing, and implant manufacturing. SLA 3D printing is also used to produce accurate prototypes of parts, even those with complex shapes, at an affordable cost to test their product designs or promote the finished product.

The advantage of SLA printing technology is its ability to print components with high resolution at a high speed. Many manufacturers have developed innovative SLA resin formulas with specific optical, mechanical, and thermal properties.[2] Notably, the mechanical properties of 3D-printed polymer materials are an essential factor. Many factors can affect the mechanical properties of the constructed component, for example, adding other materials to the polymer structure,[6] such as nanoparticles and fibers, to alter the material structure,[7] changing the printing direction, or adding post-printing processes such as photopolymerization and thermal treatment. Specifically, the construction orientation of the component plays a significant role.[6–8] A standard for 3D printing angles is yet to be fully established.[9,10] Therefore, it is still necessary to determine how the printing angle could affect the mechanical properties of 3D-printed materials.[11–13] In 3D printing, a large variety of polymeric materials for electronic devices such as semiconductors, electrodes, dielectrics, and sensors are possible. For sensors, actuators, and robots, photopolymer materials such as conductive/dielectric elastomeric materials and elastomers containing nanosilica are frequently employed. [14–17] Resin Castable Wax could be used as a matrix or scaffold for sensor devices.[18–22]

In this study, we investigate the effects of printing angle on the mechanical properties of a specific printing material. Samples made of Resin Castable Wax V1 are printed at different angles of 0, 45, and 90°. Then, the printed samples are tested via tension and compression tests.[14–16] The results may be useful in choosing an appropriate printing angle for Resin Castable Wax V1.

2. Materials and Methods

3D Smart Solutions Company, Vietnam, provided Resin Castable Wax V1, a liquid Resin Castable Wax with the properties shown in Table 1, which was used in this study. This material is a high-performance plastic with 20% waxy composition. It is specifically intended to produce precious and nonprecious metal jewelry casting cores. First, patterns were designed using 3D

Table 1
Properties of Resin Castable Wax V1.

Ultimate tensile strength	12 MPa
Tensile modulus	220 MPa
Elongation at break	13%
Temperature of 5% mass loss	249 °C
Ash content (TGA)	0.0–0.1%

AutoCAD software (Autodesk, San Francisco, CA, USA). Then, the designed patterns were exported into stereolithography format (STL) files. Next, they were printed using an SLA Form 3 printer (Formlabs, Somerville, MA, USA). They were employed to fabricate a pattern with a setting layer thickness of 50 μm. Default values were used for other parameters when producing the solid sample. The tensile test shape was designed on the basis of ASTM D638 type IV. For compressive tests, the sample shape was designed on the basis of ASTM D695 and samples were fabricated as solid cylinders with a diameter of 12.7 mm and a length of 25.4 mm. Five patterns were printed for each at 0, 45, and 90° (Figs. 1 and 2) with a printing time of 78 min, 195 layers, and a volume of 1.2 ml. After printing, the models were washed in IPA solution and dried with UV radiation with temperature gradually increasing to the threshold of 60 °C over 30 min. The steps after printing are washing, the removal of parts, the removal of supports, and curing.

Tensile and compressive tests were performed on samples with different printing angles to evaluate the effects of print orientation on the mechanical properties. In this study, the Shimadzu testing machine with a load capacity of 10 kN (Shimadzu Nakagyo, Kyoto, Japan) was used to measure tensile and compressive strengths, and it was run at a constant speed of 1.3 mm/min. The sample was clamped on the machine with a gauge length of 50 mm at room temperature. The upper clamp was moved upward until the model broke.

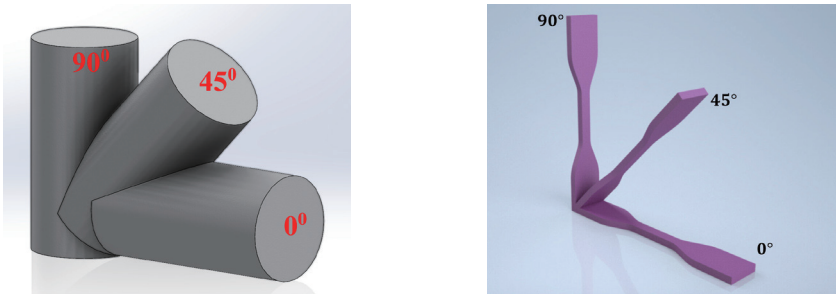

(a) (b)

Fig. 1. (Color online) Different printing angles for testing: (a) compressive and (b) tensile samples.

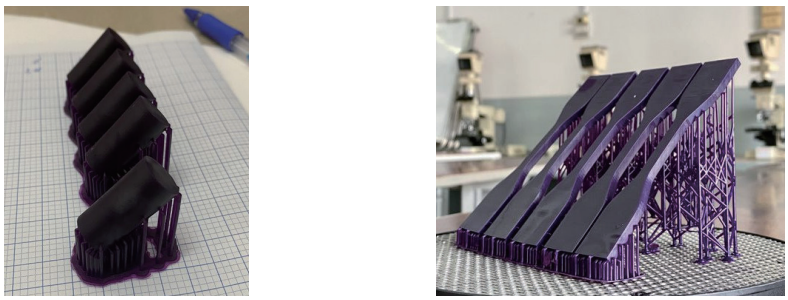

(a) (b)

Fig. 2. (Color online) Samples printed at the angle of 45°: (a) compressive and (b) tensile samples.

3. Results and Discussion

3.1 Tensile strength

The stress–strain curves of samples printed at different angles are shown in Fig. 3. Figure 4 presents the maximum tensile load at different printing angles, while Fig. 5 shows the ultimate tensile strength (UTS) calculated from the results in Fig. 4. The UTS is calculated to be 19.04, 20.72, and 23.13 MPa for printing angles of 0, 45, and 90°, respectively. The UTS gradually increases as the printing angle is increased from 0 to 90°. At the printing angle of 0°, the UTS reaches the minimum value of 19.04 MPa because the directions of the printed layers and the tensile load are parallel. This printing angle leads to a longer trajectory before a change of the printing pathway. Therefore, the boundary between different printing lines is small. In contrast, at the highest printing angle of 90°, the UTS attains the highest value of 23.13 MPa, which is 21.5% higher than that in the case of the printing angle of 0°. At this angle, the required trajectory before a change of the printing pathway is shorter, leading to a larger printing boundary between

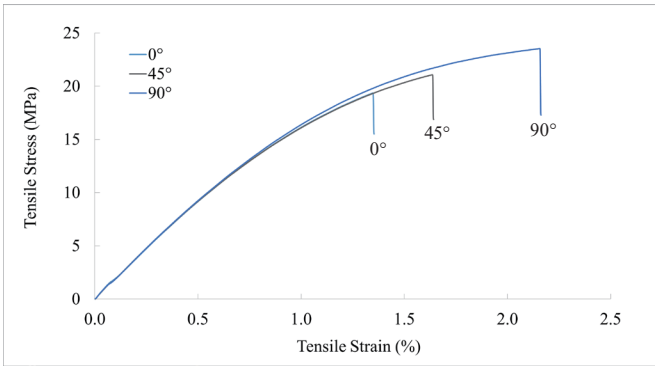

Fig. 3. (Color online) Stress–strain curves of samples printed at different angles.

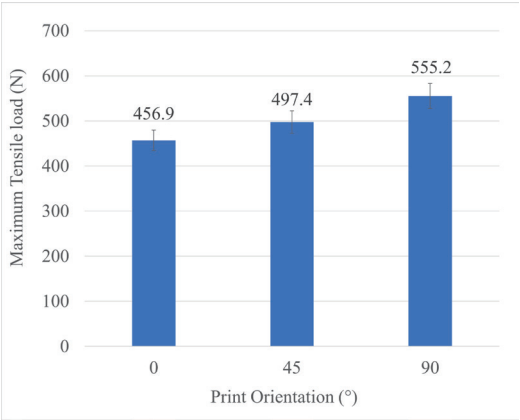

Fig. 4. (Color online) Maximum tensile loads of samples printed at different angles.

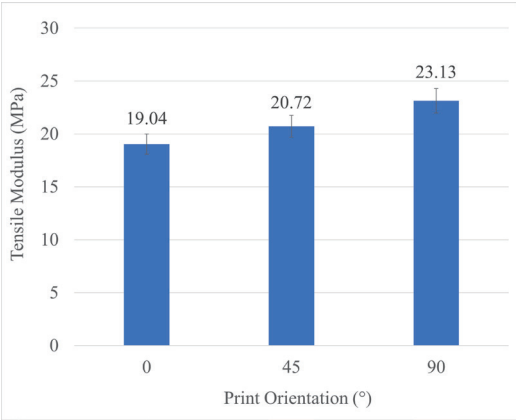

Fig. 5. (Color online) UTS values of samples printed at different angles.

different printing pathways. Notably, besides having a moderate UTS, printing at the angle of 45° requires a more significant support to fix the sample during printing, as shown in Fig. 2. Increasing the printing angle also results in a higher elongation value.

3.2 Compressive strength

In the compression test, we used a machine with a high load capacity to ensure that the sample would fail under pressure loading. The stress–strain curves during compressive testing for all models at different printing angles are indicated in Fig. 6. Figure 7 shows the maximum compressive loads of samples printed at different angles. From Fig. 7, the calculated ultimate compression strengths (UCSs) of samples are 97.89, 103.89, and 124.97 MPa for printing angles of 0, 45, and 90°, respectively. Similarly to the UTS, increasing the printing angle causes the UCS to rise owing to the change of the pattern of the samples. The UCS has the lowest value of

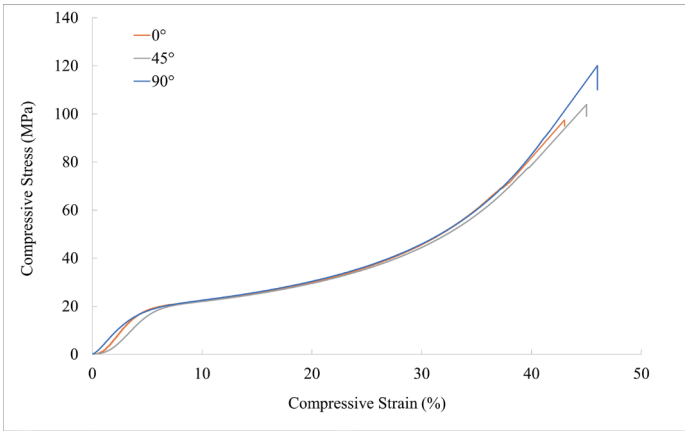

Fig. 6. (Color online) Stress–strain curves of samples printed at different angles.

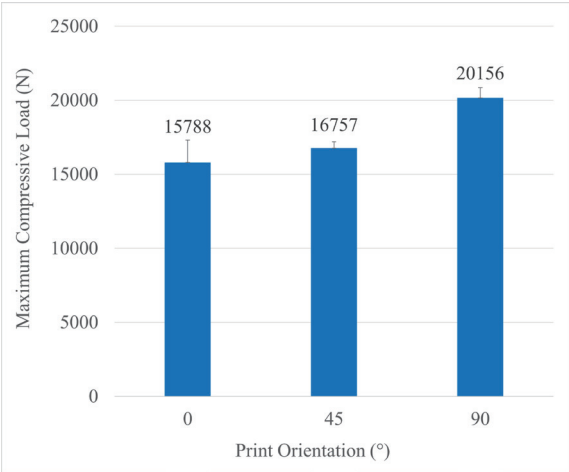

Fig. 7. (Color online) Maximum compressive loads of samples printed at different angles.

97.89 MPa at the printing angle of 0°, which is caused by the material being deposited in a direction parallel to the direction of the impact compressive load. With an increase in printing angle, the accreted material tends to be inclined towards the direction of the compressive load force. Therefore, the printed patterns tend to better resist the compressive load when the printing angle is high. At the printing angle of 90°, the UCS of the sample has the highest value of 124.97 MPa, which is 27.7% higher than the lowest value.

The printed sample withstands the highest compressive load when the material is accreted perpendicularly to the direction of the compressive load. As the compressive load increases, the print pattern slowly bulges horizontally until the compressive load reaches its highest value, resulting in the print pattern exceeding its tolerance limit and being damaged. This result explains why the maximum compressive load is the most significant value for the other two printing angles.(2) Moreover, the maximum compressive strain also increases slightly with the printing angle. Generally, the larger printing boundary at a higher printing angle is the reason for the improvement of both the UTS and the UCS.

4. Conclusions

We investigated the effects of printing angle on the mechanical properties of Resin Castable Wax V1 by stereolithography. Resin Castable Wax can be used in 3D printing as a matrix or scaffold for sensor components. Some specific results are as follows.

- Increasing the printing angle from 0 to 90° leads to improvements in both tensile and compressive strengths. The angle of 90° is the best angle for the 3D printing of Resin Castable Wax V1 materials as it results in the highest UTS and UCS. At the printing angle of 90°, the UTS is 23.13 MPa, which is 21.5% higher than that at the printing angle of 0°. Moreover, the UCS of the sample printed at the angle of 90° is 124.97 MPa, which is 27.7% higher than that at the printing angle of 0°. The maximum tensile and compressive strains are also slightly enhanced when the printing angle increases.
- The reason for the improved mechanical properties with increasing printing angle is that the material is accreted with a gradual inclination towards the direction of the load force and the larger printing boundary at a higher printing angle. Notably, at the printing angle of 45°, the sample requires more significant support to fix it during printing.
- These results can be applied to the selection of a suitable printing angle for printing Resin Castable Wax V1.

Acknowledgments

This work belongs to the project in 2024 funded by Ho Chi Minh City University of Technology and Education, Vietnam. We acknowledge Ho Chi Minh City University of Technology and Education and Material Testing Laboratory for allowing us to join the team and use the laboratory.

References

1 N. V. Ngo, K. K. Nguyen, V. T. Ngo, X. T. Vo, T. T. Nguyen, N. T. Tran, M. T. U. Tran, Q. T. Truong, and T. H. N. Pham: Proc. AMAS 2021 Advanced Mechanical Engineering, Automation, and Sustainable Development Conf. Lect. Notes Mech. Eng. (2022) 660−664. https://doi.org/10.1007/978-3-030-99666-6_95
2 J. S. Saini, L. Dowling, J. Kennedy, and D. Trimble: Proc. Inst. Mech. Eng., Part C. **234** (2020) 2279. https://doi.org/10.1177/0954406220904106
3 P. M. Dickens: J. Eng. Manuf. **209** (2002) 261. https://doi.org/10.1243/PIME_PROC_1995_209_082_02
4 T. T. Nguyen, V. T. Tran, T. H. N. Pham, V. T. Nguyen, N. C. Thanh, T. H. M. Nguyen, V. A. D. Nguyen, T. D. Nguyen, and V. T. T. Nguyen: Micromachines **14** (2023) 395. https://doi.org/10.3390/mi14020395
5 H. H. Hamzah, S. A. Shafiee, A. Abdalla, and B. A. Patel: Electrochem. Commun. **96** (2018) 27. https://doi.org/10.1016/j.elecom.2018.09.006
6 C. S. Lee, S. G. Kim, H. J. Kim, and S. H. Ahn: J. Mater. Process. Technol. **187**–**188** (2007) 627. https://doi.org/10.1016/j.jmatprotec.2006.11.095
7 V. Vega, J. Clements, T. Lam, A. Abad, B. Fritz, N. Ula, and O. S. Es-Said: J. Mater. Eng. Perform. **20** (2011) 978. https://doi.org/10.1007/s11665-010-9740-z
8 J. R. C. Dizon, A. Espera, Q. Chen, and R. C. Advincula: Addit. Manuf. **20** (2017) 44. https://doi.org/10.1016/j.addma.2017.12.002
9 A. R. Torrado and D. A. Roberson: J. Fail. Anal. Prev. **16** (2016) 154. https://doi.org/10.1007/s11668-016-0067-4
10 J. M. Montal, J. P. Sánchez, and D. Varas: Polymers **13** (2021) 1147. https://doi.org/10.3390/polym13071147
11 D. Le, C. H. Nguyen, T. H. N. Pham, V. T. Nguyen, S. M. Pham, M. T. Le, and T. T. Nguyen: J. Mater. Eng. Perfom. **137** (2023) 49087. https://doi.org/10.1007/s11665-023-07892-8
12 A. D. Leon, Q. Chen, N. B. Palaganas, P. Jerome, M. Jill, and R. C. Advincula: React. Funct. Polym. **103** (2016) 141. https://doi.org/10.1016/j.reactfunctpolym.2016.04.010
13 K. K. Yang, J. H. Zhu, C. Wang, D. S. Jia, L. L. Song, and W. H. Zhang: Comput. Mech. **61** (2018) 581. https://doi.org/10.1007/s00466-018-1537-1
14 L. Zhou, Q. Gao, J. Fu, Q. Chen, J. Zhu, Y. Sun, and Y. He: ACS Appl. Mater. Interf. **11** (2019) 23573. https://doi.org/10.1021/acsami.9b04873
15 A. D. Valentine, T. A. Busbee, J. W. Boley, J. R. Raney, A. Chortos, A. Kotikian, J. D. Berrigan, M. F. Durstock, and J. A. Lewis: Adv. Mater. **29** (2017) 1703817. https://doi.org/10.1002/adma.201703817
16 C. Tawk, M. in het Panhuis, G. M. Spinks, and G. Alici: Soft Robot. **5** (2018) 685. https://doi.org/10.1089/soro.2018.0021
17 R. L. Truby and J. A. Lewis: Nature **540** (2016) 371. https://doi.org/10.1038/nature21003
18 J. Fu, S. E. Taher, R. K. Abu Al-Rub, T. Zhang, V. Chan, and K. Liao: Adv. Eng. Mater. **24** (2022) 2101388. https://doi.org/10.1002/adem.202101388
19 A. M. Solayman: (2022). https://khalifauniversity.elsevierpure.com/en/studentTheses/characterization-of-3d-lattice-from-transition-metal-dichalcogeni-2
20 W. Liang, L. Raymond, and J. Rivas: IEEE Trans. Power Electron. **31** (2016) 52. https://doi.org/10.1109/TPEL.2015.2441005
21 S. Agrawal, H. Ray, A. Kulat, Y. Garhekar, R. Jibhakate, S. K. Singh, and H. Bisaria: Mater. Today: Proc. **72** (2023) 1231. https://doi.org/10.1016/j.matpr.2022.09.288
22 D. Thomas, L. Gallais, and J.-C. André: Appl. Sci.**13** (2023) 6844. https://doi.org/10.3390/app13116844